Modelling of an electric contact under lightning current

Jean-Baptiste Layly, Fabien Tholin, Anne Bourdon

Modelling of an Electric Contact under Lightning Current

J.B. Layly*, F. Tholin*and A. Bourdon [†]

** Onera - the French Aerospace Lab,Châtillon (F-92322), France*
[†] LPP, CNRS, Ecole Polytechnique, Palaiseau, France
Jean-baptiste.layly@onera.fr , fabien.tholin@onera.fr

Keywords: Simulation, contact resistance, out-gassing, sparking.

Abstract

Lightning stroke on aircrafts induce high current levels in aeronautic assemblies which electrical resistance is mainly concentrated in the contact interfaces between the different parts. As a consequence, the maximum Joule effects, electric fields, and hence sparking probabilities take place in the electric contacts of the aeronautic assemblies [1]. Being able to predict the behaviour of electric contacts under high current levels is then necessary to provide a better understanding on sparking and out-gassing phenomena induced by lightning stroke on aeronautic structures. The present work addresses the modelling at the microscopic scale of such electric contacts under high current levels, through a simplified geometric and physical description. 2D axisymmetric and 3D finite volume simulations are used to study simplified contact geometries and examine the current distribution dynamics, temperature increase, and phase transitions. Finally, a simple pseudo-analytical model is proposed that enables parametric studies on more complex and realistic electric contacts.

1 Introduction

The contact resistance between two conducting surfaces is a consequence of the constriction of the current lines as they cross the spots, so-called "a-spots" in the literature, where roughness micro-peaks of one surface meet those of the mating surface, as shown on Figure 1 (partly taken from [2]).

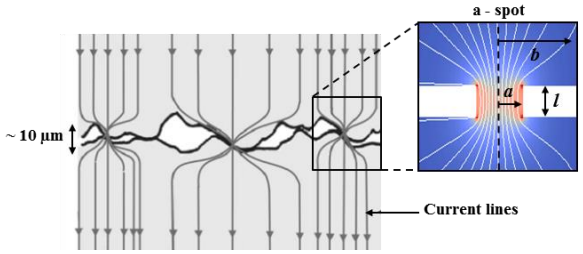

Figure 1 – Schematics of an electric contact between two surfaces on a microscopic scale [2]: three a-spots represented.

An electric contact then consists in a distribution of many a-spots in parallel, each one characterized by a constriction radius a of a few micrometres. To be able to study a realistic distribution of a-spots, a model for a single a-spot is then needed. In the first part of this study, the current distribution through a single a-spot is modelled via a 2D axisymmetric finite volume method. The electrical resistance of a single spot is then compared with the values obtained in the literature by analytical approaches. Then, the distribution of the current density and Joule heating in the spot is emphasized as well as thermal diffusion and phase transitions as the solid metal is heated up at temperatures higher than melting and boiling points. In the second part, the electrostatic interaction between different spots is addressed by means of 3D finite volume simulations. Based on these results, a simple pseudo-analytic model is finally derived in the third part of this work. It makes it possible to study the current distribution and contact resistance evolution of a cluster of many a-spots in parallel, more representative of a real contact. It is able to simulate the complete vaporization of the smallest a-spots, and the redistribution of the current from the destroyed spots to the largest ones. A parametric study is conducted with this contact model and a strong emphasis is placed on the effect of the initial spot distribution for a given contact resistance.

2 Single a-spot model

The resistance of a single a-spot can be seen as the resistance R_c (Ω) of a constriction of radius a between two cylinders of radius b (see Figure 1). R_c can be approximated by the widely used Holm's formula (1), where σ is the conductivity of the material (S m^{-1}) [3].

$$R_c = \frac{1}{2\sigma a} \tag{1}$$

This simple formula relies on the hypothesis that the constriction is axisymmetric with a zero thickness (l = 0 on Figure 1) and with perfectly spherical isopotential lines at infinity, which means that the radius b must fulfil $b \gg a$. According to (1), the resistance of many such constrictions in parallel corresponds to the resistance of a single equivalent constriction with a radius equal to $\sum a$, the sum of all the radii of the constrictions. In Holm's Theory, a distribution of many a-spots in an electric contact is then modelled by a single equivalent a-spot with radius $\sum a$. On Figure 2, the black curve shows the evolution of this constriction resistance with radius according to Holm's formula in the range 20 - 200 µm for an Al-Al contact ($\sigma = 10^7$ S m^{-1}). Moreover, for a single constriction, Holm's theory gives the norm j of the current density vector $\boldsymbol{j}$ (A m^{-2}) in the constriction (2):

$$j(r) = \frac{I}{2\pi a}\frac{1}{\sqrt{a^2 - r^2}} \tag{2}$$

I (A) is the total current flowing in the constriction and r the distance from the symmetry axis. Assuming a constant

temperature in the constriction and isotherms parallel to the isopotential lines, stationary solutions of the Fourier's law with Joule effect have been obtained that make it possible to compute the maximum temperature in the contact as a function of the potential difference, as for example the so-called φ-θ relation [3]. However, equation (2) gives an infinite current density at the periphery of the a-spot ($r = a$), which is a direct consequence of the idealized zero thickness hypothesis for the constriction, and reveals the limits of Holm's model. It is then not possible to compute a realistic unsteady current, Joule heating, and temperature distribution within Holm's theory. For this purpose, 2D axisymmetric finite volume simulations have been performed. The geometry consists in a single 2D axisymmetric constriction in cylindrical coordinates (r , z), with a thickness l = 80 µm, and a radius a varying in the range 20-200 µm. Figure 3 is a closed view of the a-spot geometry for a radius a = 200 µm, and b = 2 mm. The electrostatic current conservation equation (3) is solved thanks to the *SuperLU* solver [4], where φ is the electric potential (V):

$$\boldsymbol{\nabla} \cdot \boldsymbol{j} = -\boldsymbol{\nabla} \cdot \sigma \, \boldsymbol{\nabla}\varphi = 0 \qquad (3)$$

Dirichlet boundary conditions are imposed on the top and bottom boundaries in z = +/- 2 mm respectively to ensure a current setpoint, and a Neumann boundary is imposed at r = 2 mm. On Figure 2, the simulation results (orange curve R_s) are compared with Holm's formula (black curve R_c). In both cases the resistance decreases as the radius of the spot increases but an important difference remains. This difference is mainly due to the non-zero thickness l of the simulated spot, which resistance R_a is the association in series of two different resistances (4): A constriction resistance R_c, given by (1), and the resistance R_{cyl} of a cylinder of radius a and thickness l, given by (5):

$$R_a = R_c + R_{cyl} \qquad (4)$$

$$R_{cyl} = \frac{l}{\sigma \, \pi \, a^2} \qquad (5)$$

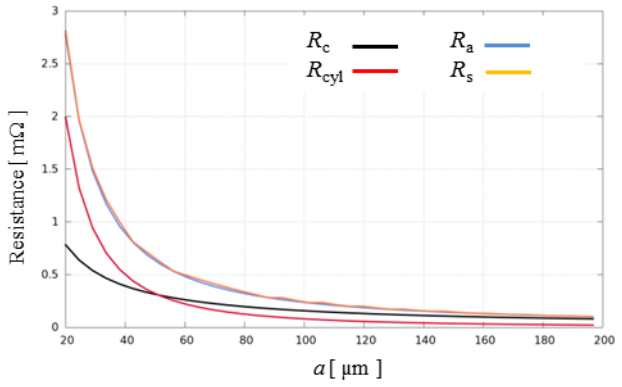

Figure 2 - Resistance of an a-spot as a function of its radius a: 2D-axisymetric simulations (R_s) and Holm's theory (R_c)

Because R_{cyl} is proportional to a^{-2}, while R_c is proportional to a^{-1}, its contribution to the total resistance R_a is dominant for small radii, as shown on Figure 2 (red curve). Then, a very good agreement is found between the numerical results and equation (4). Figure 3 shows the current streamlines and the 2D current density distribution inside the spot of radius a = 200 µm subject to a D-wave current (I = 100 kA at t = 3 µs) at the very beginning of the wave (t = 0.1 µs, I = 13 kA). Qualitatively, a good agreement is obtained with Holm's equation (2) with a current density in the constriction increasing with the radial position r, and a maximum with a sharp gradient on the rim of the spot. It appears from the different simulations performed in this study that this is a quite general geometric effect that barely depends on the exact geometry of the spot. Then the Joule effect $-\boldsymbol{j} \cdot \boldsymbol{\nabla}\varphi$ (W m^{-3}) may be computed, and used as a source term in the energy conservation equation (6), where e is the volume internal energy (J m^{-3}), λ the thermal conductivity (W m^{-1} K^{-1}), and T the temperature (K).

$$\partial_t \, e = -\boldsymbol{j} \cdot \boldsymbol{\nabla}\varphi + \boldsymbol{\nabla} \cdot \lambda \boldsymbol{\nabla} T \qquad (6)$$

$$e = \int_{T_0}^{T} \rho c_v(T) T dT + \rho(\, (Y_l + Y_g) L_f + Y_g L_v \,) \qquad (7)$$

The volume internal energy is given by equation (7), where T_0 is the room temperature, ρ is the density (kg m^{-3}), c_v the specific thermal capacity at constant volume (J kg^{-1} K^{-1}), Y_l (resp. Y_g) the mass fraction of liquid (resp. gaseous) metal and L_f (resp. L_v) the fusion (resp. vaporization) latent specific heat (J kg^{-1}). Equation (7) has been tabulated, and equations (3) and (6) are coupled by an explicit temporal scheme. This system of equations makes it possible to compute the evolution of the temperature as well as phase transitions. In order to compute the physical properties in the bi-phase regions, an assumption of homogeneous phase distribution is assumed, that results in equation (8) for the electric conductivity between phase 1 and phase 2 for example:

$$\sigma_{12} = \rho_1 Y_1 \sigma_1 + \rho_2 Y_2 \sigma_2 \qquad (8)$$

The temperature dependent thermal capacity and thermal and electric conductivities of the solid metal up to the melting point have been obtained from references [5] and [6]. However, the conductivity of the metallic vapour state is difficult to address since in the hypothesis of isochoric heating the pressure may reach thousands of bars, which would imply a fast expansion, followed by a density decrease and a metal-insulator transition in the vapour, far beyond the scope of this study [7]. As a first step, it has been assumed that the metallic vapour density and conductivity decrease fast enough so that it does not modify significantly the current distribution. Then, a conductivity of 10^4 S m^{-1}, representative of an aluminium plasma at atmospheric pressure has been considered for the gaseous phase [8]. This conductivity being much smaller than the conductivity of the solid phase (~10^7 S m^{-1}), no current flows through the gaseous phase and the vaporization of the metal of the a-spot increases its electric resistance. Because of the imposed total current flowing through the a-spot, the resistance increase due to vaporization results in a very fast increase of the Joule heating, the temperature, and then the vaporization rate itself. This thermo-electrical instability first takes place where

current density and Joule heating are the most important, which means on the rim of the a-spot. As a consequence, the vaporization dynamics results in a decrease with time of the conducting radius of the spot, defined as the radius separating the liquid phase from the gaseous phase. This important phenomenon can be observed on Figure 4: the current density is shown for the same spot and current waveform as on Figure 3, but at t = 0.7 µs, just after the beginning of the vaporization. The current density maximum is always off-axis, but not attached to the rim of the spot and closer to the centre, due to the radius decrease.

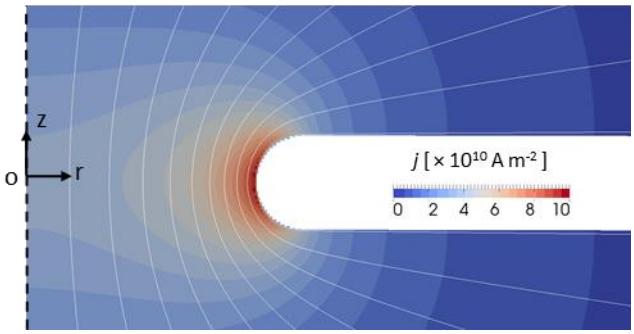

Figure 3: Current density distribution in a a-spot at the beginning of a D-wave current (t = 0.1 µs). a = 200 µm, r = 2 mm, l = 80 µm.

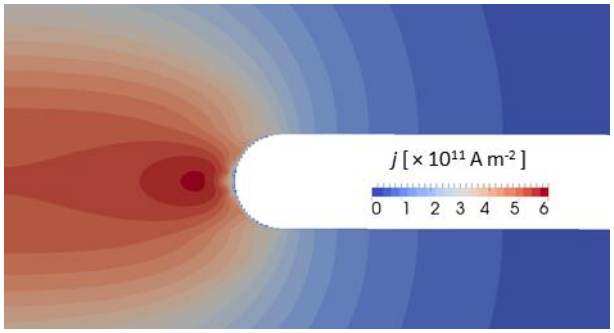

Figure 4: Current density distribution in a 200 µm a-spot at the beginning of vaporization (t = 0.7 µs) for a D-wave.

3 Multi-spot interaction

The response of a single a-spot to high current levels is closely related to the spatial distribution of the current density and the Joule effect. Then the question arises if the distribution of current density inside a-spots can be significantly modified by the presence of other spots in its neighbourhood. If the a-spots are very distant from each other relatively to their size, they can be considered as well separated from each other, and the Holm's theory is valid. On the contrary, if they are close enough, the current lines going through them will interfere. According to the Greenwood formula (9) [9], this interaction results in an additional term in the Holm's resistance formula (1) for an electric contact with n spots:

$$R_c = \frac{1}{2\sigma \sum_{i=1}^{n} a_i} + \frac{1}{\pi n^2} \sum_{i=1}^{n} \sum_{j,j\neq i}^{n} \frac{1}{s_{ij}} \qquad (9)$$

In this formula, s_{ij} (m) is the distance between a-spots i and j and a_i the radius of a-spot i. To study into more details this purely electrostatic interaction between several a-spots, 3D numerical simulations have been performed with *Code_Saturne* [10], the *EDF*'s open source CFD code, solving the current conservation equation (3) with a finite volume method. Figure 5 shows a sliced view of the current density and the current lines going through two a-spots in parallel, each spot having the same radius of 200 µm. It can be observed that the current lines between the two a-spots are influencing each other, resulting in the additional interaction resistance of Greenwood.

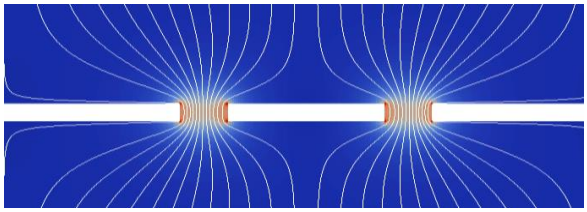

Figure 5: Sliced view of the current density flowing in two a-spots in parallel

Figure 6 shows the evolution of the resistance as a function of the separating distance. It seems clear that as soon as the distance between the spots is higher than about 20 times their radii, the resistance remains constant, meaning that the interaction becomes negligible. Same conclusion arises looking at the Joule effect distribution: when the distance between the spots is small, the current and the Joule effect distributions are modified compared to the axisymmetric distribution of an isolated spot, with reinforcement on the outer edge, and a screening effect on the inner edge. This result has also been observed on 4-spots simulations, and it could have a significant influence on the thermo-electrical response of the contact. However, since this effect disappears when the distance is about two times the radius, it seems very unlikely to occur in a real contact, or would concern only a very small number of a-spots.

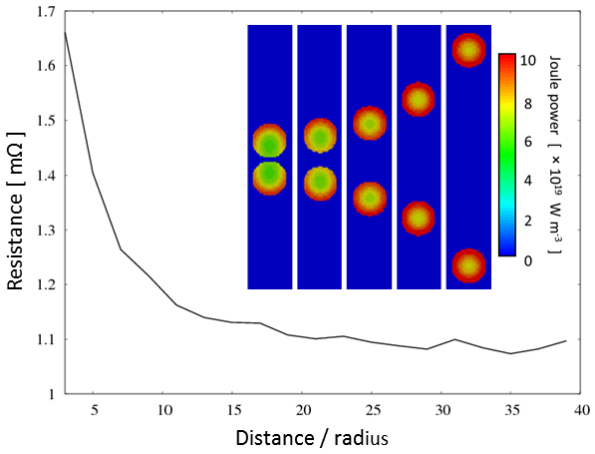

Figure 6: Total resistance of a two-spots contact and Joule power distribution as a function of the separating distance.

4 Pseudo analytic model for real contacts

Realistic electric contacts may consist in a large number of spots. It does not seem reasonable to perform detailed numerical simulations on such complex geometries with many different spatial scales. Moreover, according to previous results it is probably not necessary to get a realistic description of contacts under high current levels. The distribution in number, size and location of the a-spots, depend mainly on the mechanical load applied to the contact, and on the mechanical properties of the materials [2-3]. A mechanical model could be used to determine a realistic a-spot distribution, as performed for example by the author of [11]. This kind of method will be part of further developments, but this study is focused on the thermo-electrical constraints, and the initial a-spot distribution for a given contact is considered as an input for the simulations in the following. According to previous simulation results on multi-spot interaction, it seems reasonable to assume that all the a-spots are well isolated from each other. Then, if a current I is flowing through an electric contact, the current in each a-spot is known by solving a simple system of resistances in parallel: The current I_i going through the a-spot i is given by equation (10), with R_i the resistance of a-spot i, given by equation (4).

$$I_i = \frac{1}{R_i}\left(\frac{1}{\sum_{j=1}^{n} 1/R_j}\right) I \qquad (10)$$

To be able to take into account the complex redistribution of the current from vaporized a-spots to the remaining ones, it is important to model the fast temperature increase and phase transitions in the spots due to Joule heating. As shown previously, heating and phase transitions start on the rim of the spots due to geometric current concentration effects. It is then reasonable to consider that as soon as an a-spot reaches the boiling point, all the energy dissipated by Joule effect generates a vaporization front going from the a-spot periphery to its centre. The evolution of the radius a_i of the a-spot i is then given by the following non-linear differential equation:

$$2\pi\, a_i\, \partial_t\, a_i = -\frac{R_i(a_i)\, I_i^2}{L_v} \qquad (11)$$

A simple pseudo analytical model has been derived that solves the coupled equations (4), (10) and (11) with an explicit scheme, and considers a uniform temperature increase up to the boiling point with temperature dependent material properties (c_v, σ and λ). Figure 7 shows the evolution of the radius of a 200 µm a-spot subject to a D-wave current. The results from the pseudo-analytic model are compared to the 2D axisymmetric simulation results obtained in part 2. The definition of the radius of the a-spot in the 2D simulation is not straightforward. Contrary to the pseudo-analytic model, there is a bi-phase region in the volume of the a-spot in the 2D simulations and the vaporization front is not precisely located. Then, 2 radii have been defined: the first radius is the minimum distance from the symmetry axis where the metal is fully vaporized, which means that the volume fraction V_g of the gaseous phase is equal to 1. The second radius corresponds to the minimum distance from axis where a bi-phase region with $V_g = 0.5$ is found (half of the liquid metal is vaporized). Both models predict similar dynamics: the spot vaporization occurs very fast, in less than 0.2 µs. This is due to the increase of the resistance as the spot is vaporized, that results in an increase of the Joule effect and the vaporization rate. The two models seem to predict the starting of the vaporization at around 0.65 µs, which means at the very beginning of the D-wave. This is a strong indication that when a lightning current is flowing through an assembly with many electric contacts, current redistribution phenomena may take place on very short timescales. The differences in the radius evolution between the two models may be due to the hypothesis of vaporization front in the analytical model, but also to the fact that thermal conduction in 2D simulations act as a dissipation process that may delays the rapid collapse of the spot.

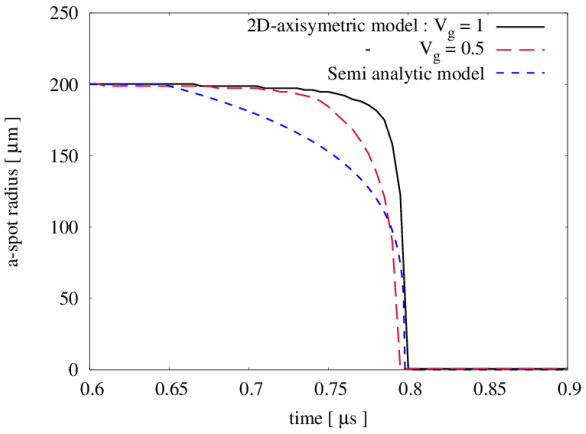

Figure 7 : Evolution of the radius of a 200 µm a-spot subject to a D-wave current: pseudo-analytic model and 2D simulations.

To study the behaviour of a cluster of many spots in parallel, several distributions have been considered that always correspond to a contact resistance of 0.1 mΩ. The different distributions differ by the number of spots N_s, and their size: Two kinds of distributions have been studied for the a-spots' radius: constant-radius distributions, where all the spots are identical and uniform distributions, where radii are evenly distributed between two values a_{min} and a_{max}, computed in order to obtain the desired contact resistance. Table 1 summarizes the different distributions simulated with the pseudo-analytic model.

Id	N_s	a_{min} [µm]	a_{max} [µm]
a	1000	0.0252	5.0497
b	100	9.736	9.736
c	100	0.08599	17.194
d	10	37.083	37.083
e	2	74.853	149.706
f	1	196.705	196.705

Table 1: a-spot distributions considered that correspond to a contact resistance of 0.1 mΩ with l=80 µm.

Figure 8 shows the evolution of the resistance (a) and the vaporized volume (b) of the 0.1 mΩ contact for the different a-spots distributions of Table 1, and assuming that a D-wave current is flowing through the contact. The complexity of the multi-spot interaction results in very different contact behaviours even if the initial contact resistance is always the same. It appears clearly that for all the distributions the vaporization takes place on very short timescales, and lead to a fast increase of the contact resistance. More surprisingly, the distributions a, b, and c exhibit almost the same dynamics, while d, e and f differ strongly. It seems that for a given contact resistance, the radius range of the distribution does not play a significant role, while the number of spots have a significant influence only in the range $1 < N_s < 10$. Contacts with small N_s seem to be able to support higher current levels, but they may lead to much more energetic outgassing phenomena at breaking point.

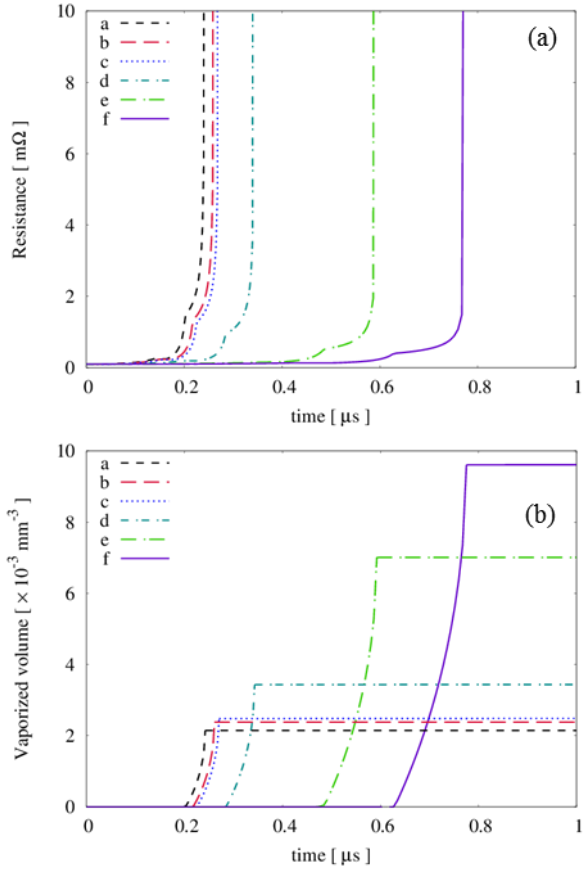

Figure 8: Evolution of the resistance (a) and volume of vaporized metal (b) in a 0.1 mΩ contact under a D-wave current for the different a-spot distributions of Table 1.

5 Conclusion

Electric contacts in aeronautic assemblies consist on a microscopic scale in many a-spots in parallel, where the current density and the Joule effect may become very important under lightning stroke conditions, leading to intense heating and metal vaporization. 2D numerical simulations on single a-spots under high currents have revealed that as soon as the vaporization of the metal takes place, the conducting radius of the a-spot decreases very fast due to a thermo-electrical instability. On the other hand, 3D numerical simulations strongly suggest that electrostatic interactions between the a-spots of a given contact have a negligible influence, and that it can be neglected for practical applications. Then, a simple pseudo-analytic model has been derived that successfully mimic the behaviour of individual a-spots, and makes it possible to consider realistic contacts with many a-spots in parallel. The evolution of the total contact resistance has been studied against different a-spots distributions for a given contact initial resistance. The number of a-spots N_s seems to have an influence when small (N_s <10), but no significant influence has been observed for higher values. This is a first prediction of the model that could be compared with experimental studies in the future. This model also allows us to predict the redistribution of the current in complex assemblies taking into account the non-linear effects occurring at high current levels. Moreover, it is able to compute macroscopic parameters, such as the electric-field, the energy dissipated in the contact, or the amount of metallic vapour produced, that could be of great interest regarding sparking and outgassing phenomena in aeronautic assemblies subject to lightning stroke.

Acknowledgements

We gratefully acknowledge the funding received toward J. B. Layly's PhD from the Plas@par Labex.

References

[1] Fustin F, Tristant F, Weydert B and Simonot D, *Fuel tank safety conditioning aspect for sparking phenomenology on metallic assemblies*, Proceedings of the International Conference on Lightning and Static Electricity, Toulouse, France, 2015

[2] Slade P G, *Electrical Contacts, Principles and Applications*, second edition, CRC Press, 2013

[3] Holm R, *Electric contact theory and application*, Fourth edition. Berlin:Springer Verlag GmbH, 1967

[4] Demmel J W, Eisenstat S C, Gilbert J R, Li X S and Liu J W H, *A supernodal approach to sparse partial pivoting*, SIAM J. Matrix Anal. Appl. **20** 720–55, 1999

[5] Haynes W M, *CRC handbook of chemistry and physics: A ready-reference book of chemical and physical data*. Boca Raton: CRC Press, 2009

[6] http://www.matweb.com

[7] Sheftman D and Krasik Ya E, *Evaluation of electrical conductivity and equations of state of non-ideal plasma through microsecond timescale underwater electrical wire explosion*, Physics of Plasmas **18**, 092704, 2011

[8] Cressault Y, Gleizes A, and Riquel G, *Properties of air–aluminum thermal plasma*, J. Phys. D: Appl. Phys. **45** 265202, 2012

[9] Greenwood J A, *Constriction resistance and the real area*, British Journal of Applied Physics **17**, pp. 1621-1632, 1966.

[10] http://www.code-saturne.org

[11] Schoft S, *Joint resistance depending on jointforce of high current aluminium joints*, Proceedings of the 22nd Conference on Electrical Contacts, pp. 502-510, 2004.